JCTC Journal of Chemical Theory and Computation

Article

pubs.acs.org/JCTC

Directional Noncovalent Interactions: Repulsion and Dispersion

Ahmed El Kerdawy,[†] Jane S. Murray,[‡,§] Peter Politzer,[‡,§] Patrick Bleiziffer,[∥] Andreas Heßelmann,[∥] Andreas Görling,[∥,⊥] and Timothy Clark*[,†,⊥,#]

[†]Computer-Chemie-Centrum, Department Chemie und Pharmazie, Friedrich-Alexander-Universität Erlangen-Nürnberg, Nägelsbachstrasse 25, 91052 Erlangen, Germany

[‡]CleveTheoComp, 1951 W. 26th Street, Suite 409, Cleveland, Ohio 44113, United States

[§]Department of Chemistry, University of New Orleans, New Orleans, Louisiana 70148, United States

[∥]Chair of Theoretical Chemistry, Department Chemie und Pharmazie, Friedrich-Alexander-Universität Erlangen-Nürnberg, Egerlandstr. 3, 91058 Erlangen, Germany

[⊥]Interdisciplinary Center for Molecular Materials, Department Chemie und Pharmazie, Friedrich-Alexander-Universität Erlangen-Nürnberg, Nägelsbachstrasse 25, 91052 Erlangen, Germany

[#]Centre for Molecular Design, University of Portsmouth, King Henry Building, King Henry I Street, Portsmouth, PO1 2DY, United Kingdom

Supporting Information

ABSTRACT: The interaction energies between an argon atom and the dihalogens Br_2, BrCl, and BrF have been investigated using frozen core CCSD(T)(fc)/aug-cc-pVQZ calculations as reference values for other levels of theory. The potential-energy hypersurfaces show two types of minima: (1) collinear with the dihalogen bond and (2) in a bridging position. The former represent the most stable minima for these systems, and their binding energies decrease in the order Br > Cl > F. Isotropic atom−atom potentials cannot reproduce this binding pattern. Of the other levels of theory, CCSD(T)(fc)/aug-cc-pVTZ reproduces the reference data very well, as does MP2(fc)/aug-cc-pVDZ, which performs better than MP2 with the larger basis sets (aug-cc-pVQZ and aug-cc-pvTZ). B3LYP-D3 and M06-2X reproduce the binding patterns moderately well despite the former using an isotropic dispersion potential correction. B3LYP-D3(bj) performs even better. The success of the B3LYP-D3 methods is because polar flattening of the halogens allows the argon atom to approach more closely in the direction collinear with the bond, so that the sum of dispersion potential and repulsion is still negative at shorter distances than normally possible and the minimum is deeper at the van der Waals distance. Core polarization functions in the basis set and including the core orbitals in the CCSD(T)(full) calculations lead to a uniform decrease of approximately 20% in the magnitudes of the calculated interaction energies. The EXXRPA+@EXX (exact exchange random phase approximation) orbital-dependent density functional also gives interaction energies that correlate well with the highest level of theory but are approximately 10% low. The newly developed EXXRPA+@dRPA functional represents a systematic improvement on EXXRPA+@EXX.

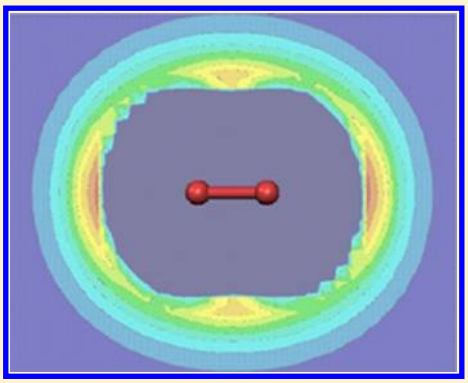

INTRODUCTION

The approximation that noncovalent intermolecular interactions can be treated as the sum of a series of isotropic two-center potentials is central to many techniques in modern computational chemistry, despite (a) being known to fail badly for Coulomb interactions[1−5] and (b) the availability of accurate multipole-based alternatives.[1,3,6−8] In fact, Price[3] has described the "assumption that the charge distribution around each atom is spherical" as a "travesty of bonding theory." There is increasing awareness that the noncovalent interactions known as σ-hole bonding, of which halogen bonding (the noncovalent binding interaction of a halogen with a Lewis base) is a subset, can be represented well by a simple anisotropic electrostatic treatment[9−19] and that even the directionality of hydrogen bonds is largely electrostatic in origin.[19−22] This has emphasized the deficiencies of isotropic atom-centered monopole (net atomic charge) models for Coulomb interactions and has led to the refinement of several force fields to account for halogen bonding.[23−26] However, even though quite sophisticated anisotropic classical theoretical models for atom−atom repulsion[27] and dispersion (van der Waals attraction)[28] have been available for some time, these interactions are almost universally represented by isotropic two-center potentials in classical modeling and also in corrections to quantum mechanical techniques that do not reproduce dispersion properly, such as have been proposed for Hartree−Fock (HF) theory,[29] density-

Received: March 8, 2013
Published: April 11, 2013

   dx.doi.org/10.1021/ct400185f | J. Chem. Theory Comput. 2013, 9, 2264−2275

functional theory (DFT),[30−32] and semiempirical molecular orbital (MO) theory.[33]

Earlier, we described a dispersion correction[34] for semiempirical MO techniques that uses the anisotropic London equation together with atomic polarizability tensors derived from a variational ansatz[35,36] with arbitrary partitioning (similar to population analysis) into atomic contributions.[37] Within this approach, the "atomic" contribution to the molecular polarizability depends strongly on the atomic orbital populations, so that atoms with strongly anisotropic electronic density distributions in their immediate vicinities should also give anisotropic contributions to the molecular electronic polarizability, and hence (via the London equation) anisotropic dispersion interactions. In this context, we note that polarizability along covalent bonds is high[22,38] and that within the linear combination of atomic orbitals (LCAO) approximation, mixing s and p orbitals leads to facile polarization along the axis of the p orbital. This is illustrated by the anisotropic polarizability tensor for the bromine atom in *p*-bromotoluene shown in ref 34 (Figure 9b). Thus, anisotropic electronic density around an atom should also lead to significantly anisotropic dispersion interactions.

σ-Holes are localized regions of positive electrostatic potential on covalently bonded atoms.[12,14−19] They result from the anisotropic electronic density distributions of the atoms.[11,15,16,18,19] There is a growing consensus that σ-hole bonding is a predominantly electrostatic-plus-polarization interaction[9−19] with a significant dispersion contribution;[39,40] the directionality of this contribution is therefore of interest. This is particularly so since directionality of noncovalent bonding has in the past usually been interpreted as being due to partial covalent character or donor−acceptor interactions.[41] This interpretation is due to the assumption that Coulomb, Pauli repulsion, and dispersion interactions are isotropic, which would mean that any directional preference can only possibly result from covalent character. It is now accepted that Coulomb interactions can be significantly directional,[9−19,42] but how significant are the directional (anisotropic) characters of Pauli repulsion and dispersion? We now report a computational analysis designed to define the general magnitudes of their directional preferences.

We wish to avoid nonunique partitioning techniques inherent in schemes designed to decompose interaction energies into specific arbitrary contributions and have therefore used the interaction energy between three different test molecules and an argon atom as a surrogate for the sum of the dispersion and repulsion effects. This is a reasonable approximation as the neutral argon atom will have no significant long-range Coulomb interaction with the test molecule and will not polarize it. The reverse polarization (of the argon atom by the test molecule) is possible but likely to be very small. BrCl and BrF have permanent dipoles, but Br_2 does not. The polarizing effect of higher multipoles falls off rapidly with distance, so that the effect will be small. Donor−acceptor (covalent) interactions can also be ruled out because an argon atom is an extremely poor donor or acceptor. The one effect that might produce a spurious directional interaction in this system is basis set superposition error (BSSE).[43] This is likely to be largest where the basis functions of the substrate molecule are weakly occupied, which is at the position of the σ-hole.[12,17] We have therefore used diffuse-augmented basis sets for the calculations and investigated the consequences of extending the basis set in order to detect possible BSSE artifacts.

Our goals in this work are two-fold: first, to investigate the topology of the dispersion interaction hypersurface for the interaction of an argon atom with the three test molecules in the context of the above discussion and, second, to test different levels of theory to determine their abilities to reproduce these interactions accurately.

TEST SYSTEMS AND METHODS

The test molecules chosen for this study are the dihalogens Br_2, BrCl, and BrF. The bromine atoms have significantly anisotropic electronic density distributions, with increasingly positive σ-holes: Br_2, 29 kcal mol^{-1}; BrCl, 36 kcal mol^{-1}; BrF, 53 kcal mol^{-1}, calculated using the M06-2X[44]/6-311G(d) procedure. The anisotropies of the bromines and the high degrees of symmetry (and therefore structural simplicities) of these molecules make them ideal candidates for a model study such as this. An argon atom was placed at positions around the dihalogen on a planar grid with 0.5 Å spacing. The energies of the system were then calculated at the CCSD(T)(fc) and CCSD(fc),[45,46] MP4sdtq-(fc),[47] and MP2(fc)[48] levels of post Hartree−Fock *ab initio* theory using the aug-cc-pVDZ, aug-cc-PVTZ, and aug-cc-PVQZ[49] basis sets, which were also used for the DFT calculations with the M06-2X,[44] M06-2X-D3,[50] B3LYP,[51] B3LYP-D3,[52] and ωB97xD[53] functionals. In addition, we have carried out CCSD(T)(full) calculations without the frozen core approximation (see below) with an aug-cc-pCVQZ[54] basis set. We used the same basis set for all-electron density-functional calculations with the EXXRPA+ (exact-exchange random phase approximation) functional,[55−59] a recently developed orbital-dependent exchange-correlation functional based on the adiabatic-connection fluctuation−dissipation theorem.[60,61] The EXXRPA+ exchange-correlation energy is evaluated post-SCF from Kohn−Sham orbitals and eigenvalues. The latter are obtained either from a self-consistent exact-exchange-only (EXX) Kohn−Sham calculation (EXXRPA+@EXX[55]) or from a self-consistent Kohn−Sham calculation that also takes into account a correlation potential at the level of the direct random phase approximation (dRPA) in addition to the exact exchange potential (EXXRPA+@dRPA[62]). See the Supporting Information for technical details and further information on the EXXRPA+@EXX and EXXRPA+@dRPA computations. The dihalogens were fixed at their ωB97xD[53]/aug-cc-pVDZ optimized geometries. The same geometries and grid points were used at the different computational levels so that the results are directly comparable. Calculations were performed with the Gaussian 09 series of programs[63] except for the CCSD(T)(full)/aug-cc-pCVQZ and EXXRPA calculations, which were carried out with the development version of the Molpro quantum chemistry package.[64] D3 corrections were applied using Grimme's program.[65] Comparisons were also performed with a variety of DFT procedures having implicit or explicit corrections for dispersion. In this case, the integration grid was set to its finest value in Gaussian (grid = ultrafine) in order to avoid small oscillations in the interaction energy over the grid of argon-atom positions. All procedures used are listed in Table 1.

RESULTS AND DISCUSSION

Figure 1 shows contour plots of the interaction energies obtained at the CCSD(T)(fc)/aug-cc-pVQZ level for the three dihalogens. In Figure S1 of the Supporting Information, these results are compared with CCSD(T)(fc) calculations with two smaller basis sets, aug-cc-pVTZ and aug-cc-pVDZ. The plots for the

Table 1. Procedures Used in This Study

level of theory/functional	basis set(s)
CCSD(T)(full)[45,46]	aug-cc-pCVQZ[54]
CCSD(T)(fc)[45,46]	
CCSD(fc)[45]	
MP4sdtq(fc)[47]	
MP4sdq(fc)[47]	
MP2(fc)[48]	aug-cc-pVDZ[49]
M06-2X[44]	aug-cc-pVTZ[49]
M06-2X-D3[50]	aug-cc-pVQZ[49]
B3LYP[51]	
B3LYP-D3[52]	
ωB97xD[53]	
EXXRPA+@EXX[51−55]	aug-cc-pCVQZ[54]
EXXRPA+@dRPA[62]	

three different basis sets are very similar. The interaction energies at the minima are more negative for the two larger ones. This rules out an anisotropic BSSE effect and suggests that the binding interaction is predominantly dispersion because it is more favorable for the two larger basis sets, which are able to reproduce correlation effects more completely with CCSD(T)(fc) than the smaller one.

The plots show two types of minima: (1) collinear with the covalent bond and (2) an equatorial belt around the center of the molecule. The collinear minima are deepest for bromine and become less favorable on going from bromine to chlorine to fluorine, although they are discernible for all three halogens. If only the bromine collinear minimum is considered, it is strongest for BrF and becomes less favorable for BrCl and least for Br_2.

Note that the collinear minima are not purely due to dispersion for BrF and BrCl, which have permanent dipoles and can therefore polarize the argon atom. The trends among the halogens are exactly the same as are found for the strengths of σ-holes,[11−17] so that we can hypothesize that the high polarizability component collinear with the dihalogen bond is associated with the partially occupied p orbital in this direction, and hence with facile s/p mixing as a polarization mechanism. This hypothesis is supported by the calculated (MP2/aug-cc-pVTZ) molecular polarizability tensors for the dihalogens (Table 2). The enhanced

Table 2. MP2/aug-cc-pVTZ Calculated Polarizability Tensors (au)[a]

	polarizability tensor components	
molecule	α_{zz}	α_{xx} (=α_{yy})
Br_2	60.55	35.72
BrCl	50.35	30.21
BrF	28.08	21.42

[a]The dihalogen bond is oriented in the z direction.

polarizability in the bond (z-) direction is partly due to the molecular shape but also to the diminished occupancy of the bromine $4p_z$-orbital compared to the $4p_x$ and $4p_y$.

A further effect that is evident from Figure 1 is the "polar flattening"[11,17−19,66−68] of the halogen atoms, especially bromine. If we define the extent of the bromine atom as the distance between its nucleus and the zero-interaction-energy contour, we find that it is 10−15% smaller in the direction collinear with the bond than perpendicular to it. This effect has long been known[11,17−19,66−68] and was probably the first real indication of the reason behind halogen bonding. It means, however, that the repulsive component of, for instance, a Lennard-Jones potential[69] should not be isotropic in this case.[27] The standard isotropic Lennard-Jones potential V_{L-J} between an atom X_i situated at the grid point $\mathbf{r}_i$ and atom X_j at $\mathbf{r}_j$ is defined as

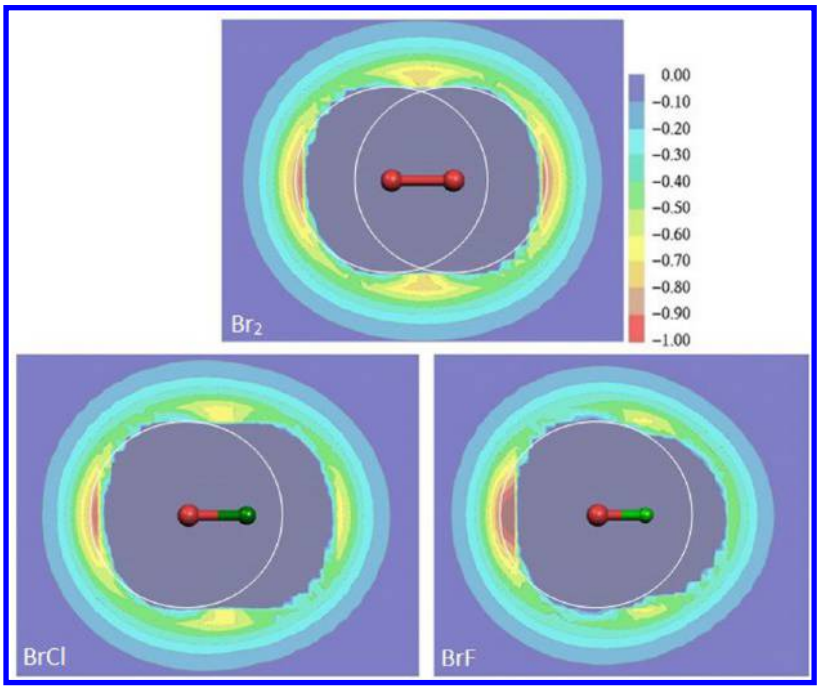

Figure 1. Contour maps of the calculated CCSD(T)(fc)/aug-cc-pVQZ Born−Oppenheimer interaction energies between an argon atom and Br_2, BrCl, and BrF. The color scale (interaction energies in kcal mol^{-1}) is the same for all plots and is shown on the right. The central repulsive area (all interaction energies larger than zero) is colored gray-blue. The white circles are for guidance and are centered on the bromine atoms.

$$V_{L-J} = 4\varepsilon_{i-j}\left[\left(\frac{R_{i-j}}{r_{ij}}\right)^{12} - \left(\frac{R_{i-j}}{r_{ij}}\right)^{6}\right] \quad (1)$$

where R_{i-j} is the sum of the van der Waals radii of atoms X_i and X_j, ε_{i-j} is the well depth, and r_{ij} is the distance between points r_i and r_j. Figure 2 shows the calculated interaction energy between Br_2 and Ar using typical Lennard-Jones parameters taken from the literature (ε_{Br-Ar} = 0.2842 kcal mol^{-1} and R_{Ar-Br} = 3.51 Å).[70] The interaction energy of the argon atom with each of the bromines corresponds to eq 1.

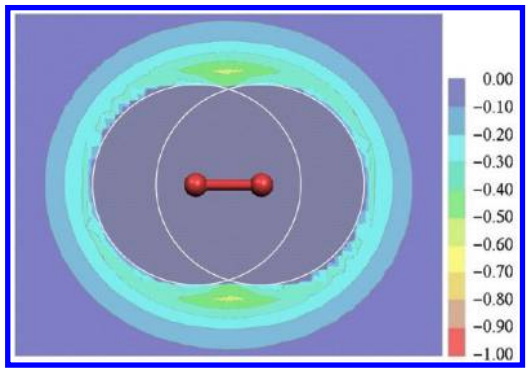

Figure 2. Contour map of the calculated Born−Oppenheimer interaction energies between an argon atom and Br_2 using standard two-center Lennard-Jones potentials with parameters taken from ref 70. The color scale (interaction energies in kcal mol^{-1}) is shown on the right. The central repulsive area (all interaction energies larger than zero) is colored gray-blue. The white circles are for guidance and are centered on the bromine atoms.

The standard two-center Lennard-Jones potential can reproduce the equatorial binding position but not the minima collinear with the Br−Br bond, which are completely absent (but see the discussion of B3LYP-D3 below). Although the absolute error of the interaction energy for these minima is only approximately 1 kcal mol^{-1}, the nature of the van der Waals potential energy hypersurface is completely different from that shown in Figure 1. Neither the angular dependence of the binding energy nor the positions of the deepest minima are reproduced by the standard two-center potential.

Polar flattening, mentioned above, requires that R_{i-j} be a function of the angle between the covalent bond and the grid point being considered. However, the most important feature of Figure 1 in the present context is that it cannot be reproduced using a two-center isotropic potential such as the Lennard-Jones, eq 1, to obtain the sum of the interaction energies of each halogen atom with the argon. The reason is that for a given distance between the argon and the closer halogen atom, the corresponding distance to the farther halogen atom is a maximum when the argon is on the extension of the covalent bond between the halogens. Accordingly, the sum of the interaction energies of the argon with the two halogens will be least negative along the extension of the bond, not most negative there as shown in Figure 1.

Either or both the well depth, ε and R_{i-j}, must therefore be anisotropic in order to be able to reproduce the plots shown in Figure 1. Figure 2 shows that the steep distance dependence of the Lennard-Jones 12−6 potential means that it predicts essentially isotropic dispersion interactions around the atoms of Br_2. The only deviations are in the bridging position where both atoms are within van der Waals distance of the argon. Overall, the differences between the interaction-energy hypersurfaces shown in Figures 1 and 2 are small in absolute magnitude (because the dispersion energy itself is small) but disturbingly large in the characters of the hypersurfaces. The importance of dispersion lies in the large numbers of interactions in bigger systems, so that deviations like the ones shown can become very significant. It is therefore important to assess the performance of levels of theory more economical than CCSD(T)(fc) in reproducing the interactions of the dihalogens with argon. The raw data for the reference CCSD(T)(fc) calculations are included in the Supporting Information (S2) so that other methods can be tested.

Møller−Plesset Methods and CCSD(fc). Table 3 shows the results of a statistical analysis of the Born−Oppenheimer interaction energies calculated for the three systems at the *ab initio* (post Hartree−Fock) computational levels outlined in Table 1; each of these procedures is compared to CCSD(T)(fc)/aug-cc-pVQZ. The results for the three dihalogens are largely very similar. Many patterns can be recognized. The CCSD(T)-(fc) results depend quite strongly on the basis set. Aug-cc-pVTZ reproduces aug-cc-pVQZ closely in all three examples (R^2 = 0.985−0.993, slopes = 0.966−1.001, constants = −0.003 to −0.007), but aug-cc-pVDZ deviates quite strongly (R^2 = 0.837−0.891, slopes =0.786−0.830, constants = −0.019 to −0.028). The CCSD(fc) results deviate significantly and depend more strongly on the basis set than CCSD(T)(fc). The general conclusion for these three systems is that decreasing the basis set to aug-cc-pVTZ is preferable to neglecting the perturbational triples correction.

As a more economical alternative to CCSD(T)(fc), MP4sdtq-(fc) gives very good results. The triples contribution is important; neglecting it leads to significantly worse agreement with the reference procedure, as also observed for coupled cluster calculations. Interestingly, MP4sdtq(fc)/aug-cc-pVTZ gives the most balanced (largest positive and negative errors are most similar, slope is closest to one) agreement with CCSD(T)(fc)/aug-cc-pVQZ. MP4sdtq(fc) binding energies are slightly too negative with the quadruple-ξ basis set and too positive with the double-ξ.

These trends are reflected even more strongly in the MP2 results, which are perhaps the most interesting. MP2 with large basis sets overestimates the dispersion contributions. The effects inherent in the MP2 correction have been discussed by Merz et al.,[71] Cybulski et al.,[72] and Chalasinski and Szczesniak.[73] Despite the binding energies being too high (interaction energies too negative), MP2 can give excellent results at a very reasonable cost as long as the basis set is not too large. The same effect can be achieved using SCS-MP2.[74] Figure 3 compares the MP2 results for Br_2:Ar, using the three basis sets, with the reference procedure. The qualitative binding pattern is correct in each case, and the absolute agreement is very good for the smallest basis set (R^2 = 0.971, slope = 0.983, constant = −0.022, error range −0.082 to 0.131 kcal mol^{-1}). This balanced performance is also found for BrCl:Ar at the MP2/aug-cc-pVDZ level; for BrF, however, MP2/aug-cc-pVTZ performs somewhat better than the smallest basis set. Clearly, reducing the MP2 correlation correction by limiting the extent of the virtual space results in a "Pauling Point,"[75] at which canceling errors lead to the correct result. The present data for only three dihalogens are not sufficient to suggest that this is a general conclusion but do point to a potentially useful observation.

Table 3. Statistical Analyses of the Performance of Each Procedure Relative to CCSD(T)(fc)/aug-cc-pvQZ[a]

level		R^2	slope	constant	RMSD	MSE	extreme errors +ve	extreme errors −ve
				Br_2:Ar				
CCSD(T)(fc)	TZ	0.987	0.995	−0.003	0.025	−0.002	0.149	−0.047
	DZ	0.837	0.786	−0.027	0.091	0.018	0.447	−0.061
CCSD(fc)	QZ	0.922	0.764	−0.004	0.084	0.046	0.348	0.001
	TZ	0.871	0.783	−0.006	0.090	0.040	0.457	−0.002
	DZ	0.648	0.641	−0.028	0.138	0.049	0.660	−0.048
MP4sdtq(fc)	QZ	0.996	1.072	0.001	0.026	−0.014	0.000	−0.114
	TZ	0.996	1.055	−0.002	0.023	−0.014	0.053	−0.083
	DZ	0.865	0.814	−0.027	0.082	0.013	0.397	−0.064
MP4sdq(fc)	QZ	0.923	0.764	−0.004	0.084	0.047	0.346	0.001
	TZ	0.875	0.786	−0.006	0.089	0.040	0.450	−0.002
	DZ	0.661	0.649	−0.027	0.135	0.047	0.644	−0.049
MP2(fc)	QZ	0.964	1.269	0.002	0.097	−0.055	−0.001	−0.424
	TZ	0.989	1.236	0.000	0.077	−0.050	−0.001	−0.242
	DZ	0.971	0.983	−0.022	0.041	−0.019	0.131	−0.082
				BrCl:Ar				
CCSD(T)(fc)	TZ	0.993	1.001	−0.005	0.017	−0.006	0.130	−0.046
	DZ	0.891	0.830	−0.028	0.064	0.002	0.321	−0.070
CCSD(fc)	QZ	0.942	0.750	−0.006	0.071	0.039	0.307	0.001
	TZ	0.915	0.776	−0.010	0.068	0.030	0.399	−0.003
	DZ	0.750	0.675	−0.029	0.100	0.028	0.508	−0.040
MP4sdtq(fc)	QZ	0.998	1.069	0.002	0.019	−0.011	0.000	−0.096
	TZ	0.997	1.058	−0.004	0.021	−0.015	0.050	−0.070
	DZ	0.908	0.858	−0.027	0.058	−0.002	0.286	−0.075
MP4sdq(fc)	QZ	0.942	0.749	−0.005	0.071	0.039	0.302	0.001
	TZ	0.917	0.777	−0.010	0.068	0.030	0.392	−0.003
	DZ	0.760	0.682	−0.029	0.098	0.027	0.494	−0.040
MP2(fc)	QZ	0.980	1.257	0.004	0.073	−0.041	−0.001	−0.345
	TZ	0.992	1.235	−0.001	0.065	−0.042	0.000	−0.219
	DZ	0.977	1.026	−0.021	0.040	−0.026	0.111	−0.110
				BrF:Ar				
CCSD(T)(fc)	TZ	0.985	0.966	−0.007	0.024	−0.001	0.201	−0.061
	DZ	0.867	0.791	−0.019	0.075	0.015	0.472	−0.038
CCSD(fc)	QZ	0.948	0.776	−0.003	0.066	0.034	0.358	0.000
	TZ	0.902	0.764	−0.009	0.074	0.030	0.517	−0.006
	DZ	0.712	0.644	−0.019	0.113	0.039	0.695	−0.019
MP4sdtq(fc)	QZ	0.997	1.077	0.002	0.022	−0.011	0.000	−0.153
	TZ	0.992	1.034	−0.006	0.023	−0.011	0.066	−0.118
	DZ	0.892	0.833	−0.019	0.066	0.009	0.392	−0.047
MP4sdq(fc)	QZ	0.957	0.797	−0.002	0.060	0.031	0.312	0.000
	TZ	0.915	0.785	−0.008	0.068	0.027	0.472	−0.009
	DZ	0.736	0.664	−0.019	0.108	0.036	0.656	−0.021
MP2(fc)	QZ	0.986	1.180	0.005	0.051	−0.025	0.000	−0.395
	TZ	0.998	1.125	−0.001	0.034	−0.022	0.000	−0.177
	DZ	0.950	0.913	−0.012	0.044	0.002	0.262	−0.042

[a]Energies are given in kcal mol^{-1}. R^2 is the squared correlation coefficient between the two sets of energies. RMSD is the root-mean-square deviation between them, and MSE is the mean signed error. The extreme errors are the most positive and most negative differences between the procedure being considered and the reference ($E_{current} - E_{reference}$). Only the bound points (those with an interaction energy less than zero at the reference level) are included in the statistics. The aug-cc-pVDZ, aug-cc-pVTZ, and aug-cc-pVQZ basis sets[49] are represented by the abbreviations DZ, TZ, and QZ, respectively. The columns labeled "slope" and "constant" give the slope a and constant c in the regression equation $y = ax + c$, where x is the reference procedure and y is the one being compared.

The Effect of Core Polarization and Correlation. Although CCSD(T)(fc)/aug-cc-pVQZ calculations could be expected to give very high quality interaction energies for this system, one uncertainty in the standard CCSD(T)(fc) methodology remains uncertain: the effect of the nonvalence (core) orbitals. Both polarization of the core orbitals and electron correlation with or between them could affect the results for systems with heavy halogens and argon quite significantly. We therefore performed a second set of CCSD(T)(full) calculations in which the basis set (aug-cc-pCVQZ[50]) contained core polarization functions and the core orbitals were included in the coupled cluster treatment. The results are shown in Table 4.

The effect of core polarization and correlation is moderate but significant. The frozen-core calculations give 10−20% more

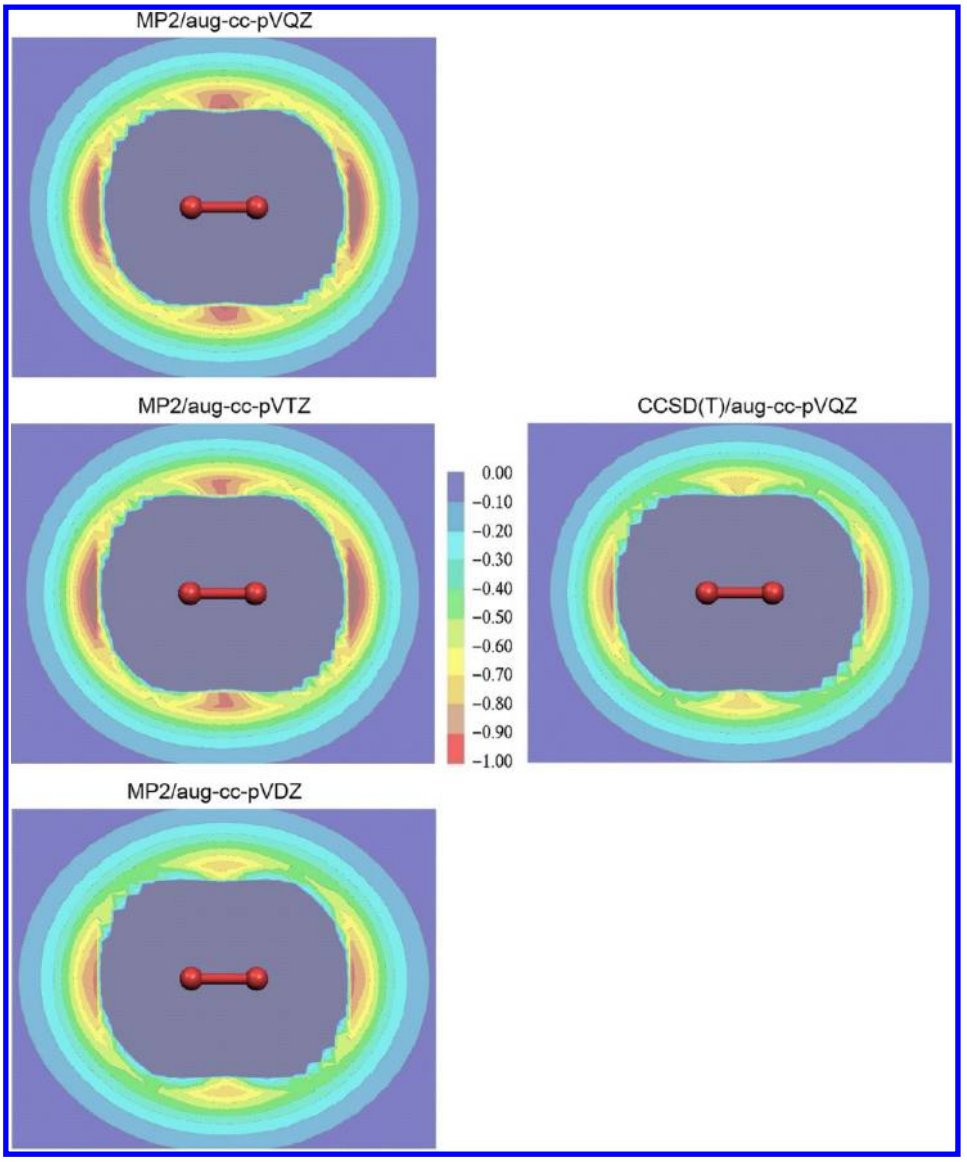

Figure 3. Comparison of the MP2 results with the CCSD(T)(fc)/aug-cc-pVQZ reference energies (right). The color code and conventions used in the plots are the same as those used in Figures 1 and 2.

Table 4. Statistical Analyses of the Effects of Adding Core Polarization Functions to the Basis Set and Including the Core Orbitals in the Coupled Cluster Calculation[a]

						extreme errors	
system	R^2	slope	constant	RMSD	MSE	+ve	−ve
			CCSD(T)(fc)/aug-cc-pVQZ				
Br_2:Ar	0.987	1.202	−0.005	0.060	−0.040	−0.001	−0.186
BrCl:Ar	0.991	1.112	−0.002	0.033	−0.019	0.000	−0.137
BrF:Ar	0.995	1.157	−0.002	0.039	−0.024	0.000	−0.173

[a]The analysis shows the statistics of the bound points for CCSD(T)(fc)/aug-cc-pVQZ relative to CCSD(T)(full)/aug-cc-pCVQZ. Energies are given in kcal mol^{-1}. R^2 is the squared correlation coefficient between the two sets of energies. RMSD is the root-mean-square deviation between them, and MSE is the mean signed error. The extreme errors are the most positive and most negative differences between the level being considered and the reference ($E_{current} - E_{reference}$). Only the bound points (those with an interaction energy less than zero at the reference level) are included in the statistics. The columns labeled "slope" and "constant" give the slope a and constant c in the regression equation $y = ax + c$, where x is the reference procedure and y is the one being compared.

negative dispersion energies than the higher level. The correlations are, however, all good (R^2 between 0.987 and 0.995), and the regression lines all pass very close to the origin. Thus, the general features of the interaction-energy maps remain the same but the magnitudes of the binding energies are somewhat decreased at the higher level of theory.

Density-Functional Theory. Table 5 shows a statistical analysis for the DFT levels of theory compared to the reference CCSD(T)(fc)/aug-cc-pVQZ results. This level was used as a

dx.doi.org/10.1021/ct400185f | J. Chem. Theory Comput. 2013, 9, 2264−2275

Table 5. Statistical Analyses of the Performance of Each DFT Procedure Relative to the Reference CCSD(T)(fc)/aug-cc-pVQZ[a]

level		R^2	slope	constant	RMSD	MSE	extreme errors +ve	extreme errors −ve
				Br_2:Ar				
B3LYP	QZ	0.177	−0.502	0.010	0.521	0.330	1.791	0.006
	TZ	0.177	−0.500	0.006	0.518	0.326	1.779	0.006
	DZ	0.138	−0.420	−0.001	0.488	0.301	1.737	0.007
B3LYP-D3	QZ	0.765	0.660	0.009	0.136	0.081	0.752	0.001
	TZ	0.766	0.661	0.005	0.133	0.078	0.756	0.001
	DZ	0.835	0.742	−0.002	0.105	0.053	0.663	−0.009
B3LYP-D3(bj)	QZ	0.922	0.756	0.011	0.095	0.063	0.377	0.001
	TZ	0.924	0.757	0.007	0.092	0.059	0.380	0.001
	DZ	0.955	0.837	−0.001	0.063	0.034	0.287	−0.011
M06-2X	QZ	0.642	0.440	−0.057	0.154	0.062	0.418	−0.059
	TZ	0.758	0.515	−0.044	0.137	0.059	0.371	−0.048
	DZ	0.958	0.805	0.021	0.084	0.063	0.209	−0.087
M06-2X-D3	QZ	0.620	0.437	−0.080	0.149	0.040	0.409	−0.063
	TZ	0.740	0.512	−0.067	0.130	0.037	0.356	−0.052
	DZ	0.960	0.802	−0.001	0.069	0.041	0.195	−0.089
ωB97XD	QZ	0.052	0.185	−0.032	0.285	0.141	1.126	0.001
	TZ	0.108	0.262	−0.032	0.261	0.125	1.092	0.000
	DZ	0.448	0.490	−0.025	0.183	0.084	0.791	−0.014
				BrCl:Ar				
B3LYP	QZ	0.254	−0.513	−0.003	0.425	0.265	1.536	0.005
	TZ	0.254	−0.511	−0.006	0.422	0.261	1.527	0.005
	DZ	0.194	−0.425	−0.012	0.398	0.241	1.483	0.005
B3LYP-D3	QZ	0.910	0.711	0.004	0.088	0.055	0.546	0.000
	TZ	0.913	0.713	0.000	0.086	0.051	0.541	0.000
	DZ	0.940	0.799	−0.005	0.062	0.030	0.450	−0.012
B3LYP-D3(bj)	QZ	0.971	0.810	0.007	0.061	0.041	0.259	0.000
	TZ	0.974	0.812	0.004	0.057	0.037	0.254	0.000
	DZ	0.983	0.899	−0.001	0.034	0.017	0.168	−0.014
M06-2X	QZ	0.740	0.481	−0.078	0.113	0.014	0.348	−0.085
	TZ	0.846	0.581	−0.063	0.093	0.012	0.330	−0.074
	DZ	0.961	0.848	0.007	0.055	0.034	0.168	−0.126
M06-2X-D3	QZ	0.717	0.479	−0.099	0.114	−0.007	0.327	−0.094
	TZ	0.832	0.579	−0.084	0.094	−0.009	0.309	−0.082
	DZ	0.963	0.847	−0.014	0.045	0.013	0.150	−0.129
ωB97XD	QZ	0.060	0.171	−0.038	0.230	0.109	0.980	−0.001
	TZ	0.155	0.268	−0.037	0.205	0.093	0.942	−0.001
	DZ	0.550	0.500	−0.028	0.142	0.061	0.643	−0.015
				BrF:Ar				
B3LYP	QZ	0.089	−0.272	0.026	0.382	0.235	1.520	0.001
	TZ	0.091	−0.272	0.022	0.379	0.231	1.508	0.001
	DZ	0.049	−0.193	0.021	0.360	0.217	1.481	0.006
B3LYP-D3	QZ	0.866	0.690	0.007	0.099	0.058	0.660	−0.003
	TZ	0.865	0.690	0.004	0.097	0.055	0.698	−0.003
	DZ	0.904	0.769	0.002	0.078	0.041	0.573	−0.004
B3LYP-D3(bj)	QZ	0.920	0.811	0.018	0.077	0.049	0.383	−0.003
	TZ	0.930	0.811	0.014	0.073	0.045	0.370	−0.003
	DZ	0.948	0.889	0.013	0.056	0.031	0.344	−0.014
M06-2X	QZ	0.773	0.657	−0.009	0.108	0.048	0.363	−0.102
	TZ	0.869	0.719	−0.001	0.090	0.046	0.319	−0.053
	DZ	0.924	0.903	0.068	0.100	0.084	0.258	−0.273
M06-2X-D3	QZ	0.759	0.651	−0.027	0.104	0.031	0.355	−0.116
	TZ	0.859	0.713	−0.019	0.085	0.029	0.310	−0.067
	DZ	0.921	0.897	0.050	0.087	0.067	0.250	−0.286
ωB97XD	QZ	0.077	0.225	−0.020	0.240	0.108	1.153	0.001
	TZ	0.142	0.286	−0.023	0.218	0.095	1.022	0.001
	DZ	0.371	0.468	−0.011	0.175	0.076	0.931	−0.003

[a]Energies are given in kcal mol^{-1}. R^2 is the squared correlation coefficient between the two sets of energies. RMSD is the root-mean-square deviation between them, and MSE is the mean signed error. The extreme errors are the most positive and most negative differences between the level being

dx.doi.org/10.1021/ct400185f | J. Chem. Theory Comput. 2013, 9, 2264−2275

Table 5. continued

considered and the reference ($E_{current} - E_{reference}$). Only the bound points (those with an interaction energy less than zero at the reference level) are included in the statistics. The columns labeled "slope" and "constant" give the slope a and constant c in the regression equation $y = ax + c$, where x is the reference procedure and y is the one being compared.

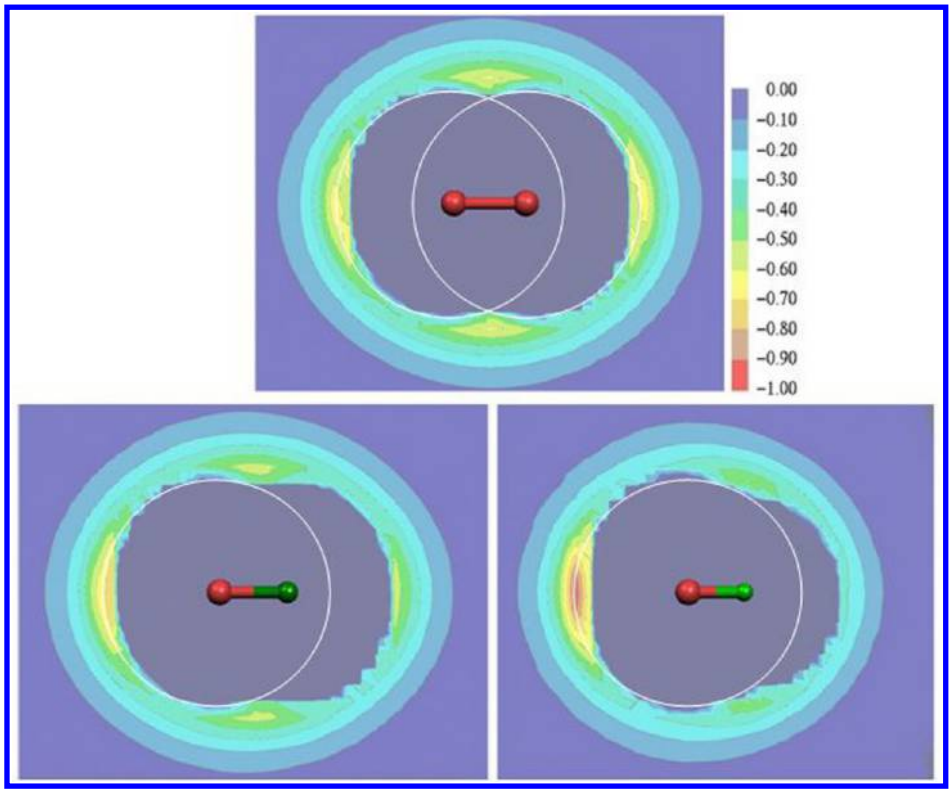

Figure 4. B3LYP-D3/aug-cc-pVDZ (with zero-damping) results for the three systems considered. The color code and conventions used in the plots are the same as those in Figures 1 and 2. The white circles are centered on the bromine atoms for guidance.

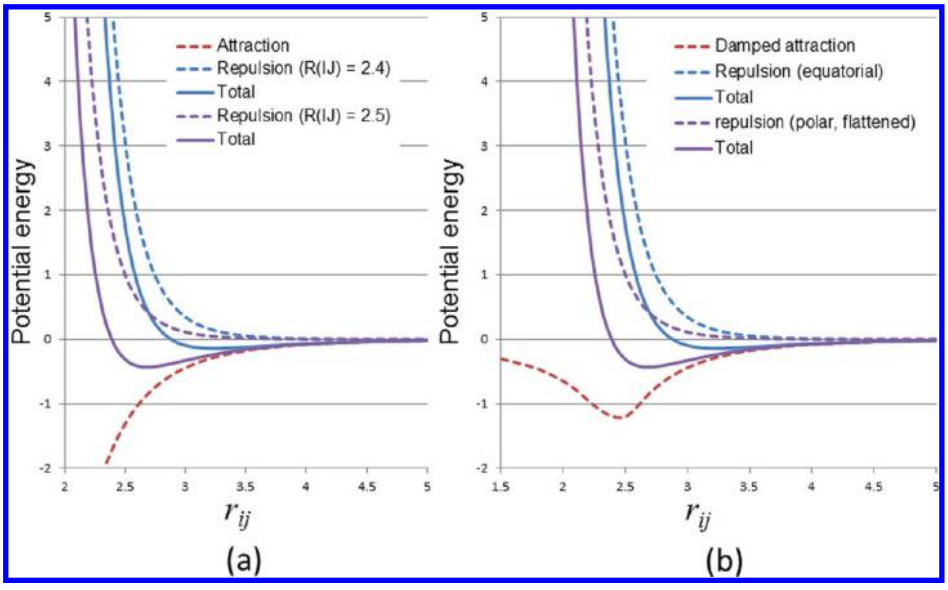

Figure 5. Schematic diagram of the effects of (a) reducing the R_{i-j} parameter for the repulsive term in a standard 12−6 Lennard-Jones potential and (b) reduced repulsion due to polar flattening in a halogen for DFT functionals with a damped dispersion potential.

reference because the core polarization functions were not included in the basis set for the DFT calculations apart from those with EXXRPA+@EXX and EXXRPA+@dRPA.

The uncorrected B3LYP results are very poor. The highest correlation coefficients found are 0.254 (for BrCl), and the slopes are all negative because B3LYP does not reproduce the dispersion energy at all.

Surprisingly, considering the discussion in the Introduction, B3LYP-D3, which uses an additional isotropic dispersion correction, reproduces the qualitative binding features well and

Table 6. Statistical Analyses of the Performances of EXXRPA+@EXX/aug-cc-pCVQZ and EXXRPA+@dRPA(full)/aug-cc-pCVQZ Density Functional Calculations Relative to CCSD(T)(full)/aug-cc-pCVQZ Calculations[a]

						extreme errors	
system	R^2	slope	constant	RMSD	MSE	+ve	−ve
			EXXRPA+@EXX(full)/aug-cc-pCVQZ				
Br_2:Ar	0.980	0.908	0.060	0.081	0.076	0.213	0.057
BrCl:Ar	0.985	0.894	0.066	0.087	0.083	0.240	0.036
BrF:Ar	0.985	0.859	−0.035	0.033	−0.015	0.242	−0.035
			EXXRPA+@dRPA(full)/aug-cc-pCVQZ				
Br_2:Ar	0.994	0.941	−0.030	0.026	−0.020	0.056	−0.032
BrCl:Ar	0.995	0.951	−0.039	0.034	−0.030	0.065	−0.053
BrF:Ar	0.993	0.916	−0.033	0.029	−0.021	0.150	−0.074

[a]Energies are given in kcal mol^{-1}. R^2 is the squared correlation coefficient between the two sets of energies. RMSD is the root-mean-square deviation between them, and MSE is the mean signed error. The extreme errors are the most positive and most negative differences between the level being considered and the reference ($E_{current} - E_{reference}$). Only the bound points (those with an interaction energy less than zero at the reference level) are included in the statistics. The columns labeled "slope" and "constant" give the slope a and constant c in the regression equation $y = ax + c$, where x is the reference procedure and y is the one being compared.

gives moderately good statistical parameters (R^2 = 0.765−0.940, slope = 0.660−0.799, constant = −0.005 to +0.009, error range = −0.012 to +0.756 kcal mol^{-1}). Figure 4 shows B3LYP-D3/aug-cc-pVDZ results for the three systems considered. In each case, B3LYP-D3 is able to reproduce the collinear minima despite the fact that isotropic potentials alone cannot do so (and B3LYP itself gives no dispersion energy). The explanation of this apparent paradox lies only indirectly in the additive dispersion (R^{-6}) term used in B3LYP-D3. Polar flattening reduces the repulsion term (which is explicit in DFT) in the collinear direction so that the sum of the damped D3 correction and the repulsion can become more negative in the polar areas. Thus, Figure 4 suggests that Lennard-Jones potentials, eq 1, in which only R_{i-j} in the repulsive term is direction-dependent (and not necessarily ε_{i-j} or R_{i-j} in the attractive term) might give good results. This is illustrated in Figure 5, which shows (a) the effect of shortening R_{i-j} for the repulsive term in a standard 12−6 Lennard-Jones potential and (b) the effect of polar flattening in a DFT technique with a damped dispersion term. B3LYP-D3 binding energies are largely independent of the basis set because essentially the entire binding contribution is provided by the dispersion correction term. This does not invalidate the hypothesis that the polarizabilities of the dihalogens in the bond regions enhance dispersion collinear with the bonds. However, the polar flattening reduction of the repulsion also leads to this effect.

B3LYP-D3(bj) performs even better than B3LYP-D3, supporting the hypothesis that the damping function plays an important role in determining the performance of empirically corrected functionals. Interestingly, B3LP-D3(bj)/aug-cc-pVDZ consistently performs best for all three test cases.

The addition of a D3 term to M06-2X does not affect the results strongly, as is shown in the Supporting Information (S3). The qualitative binding topology is correct in both cases. Once again, the best results are obtained with the small basis set. Generally, the statistical performances of B3LYP-D3 and M06-2X calculations (either with or without the D3 correction) are very similar, although M06-2X usually gives more balanced maximum positive and negative errors.

The performance of ωB97XD is disappointing. It tends toward the "isotropic" binding topology shown in Figure 2 (please see the Supporting Information for contour maps of the ωB97XD results) and once more gives best agreement with the reference calculations with the smallest basis set.

Next-Generation DFT Functionals. Just how well can more advanced density-functional techniques treat this problem? We have tested the EXXRPA+@EXX and EXXRPA+@dRPA exact-exchange functionals with the largest (aug-cc-pCVQZ) basis set and compared the calculated interaction energies with those obtained with the same basis set and CCSD(T)(full) without the frozen core approximation. This comparison was chosen because EXXRPA+@EXX and EXXRPA+@dRPA consider core correlation and are therefore most directly comparable to the full CCSD(T) calculations. The results are shown in Table 6.

The EXXRPA+@EXX functional performs well. It is able to reproduce the minima and the topology of the interaction-energy hyperspaces correctly. It consistently gives 86−91% of the interaction energy with a good correlation (R^2 lies between 0.98 and 0.99). The regression lines pass very close to the origin. This performance is found consistently for all three test systems.

The newly developed EXXRPA+@dRPA functional improves on the performance of EXXRPA. R^2 is higher than 0.99 in all cases. EXXRPA+@dRPA consistently recovers 92 to 95% of the interaction energy and reproduces the topology of the interaction energy hypersurface very well. A systematic improvement in the results is visible for all three test cases. Thus, the EXXRPA+@EXX and EXXRPA+@dRPA functionals are able to reproduce the interaction energies in these difficult systems remarkably well, and above all consistently, at a fraction of the cost of the CCSD(T) calculations.

The excellent performance of EXXRPA+@dRPA is shown in Figure 6, a difference map between the CCSD(T)(full) and EXXRPA+@dRPA calculations with the aug-cc-pCVQZ basis set. The density functional calculations underestimate the binding at the collinear minima by approximately 0.06 kcal mol^{-1}.

CONCLUSIONS

Our model systems for pure dispersion interactions reveal quite strong structure in the contour maps of the interaction energies of an argon atom with the three dihalogens. Such interaction hypersurfaces cannot be reproduced using standard 12−6 Lennard-Jones atom−atom potentials but are intriguingly reproduced quite well by B3LYP-D3. The observed minima collinear with the dihalogen bond outside the bromine atoms are found with B3LYP-D3 because polar flattening allows the argon atom to approach the bromine more closely before repulsion

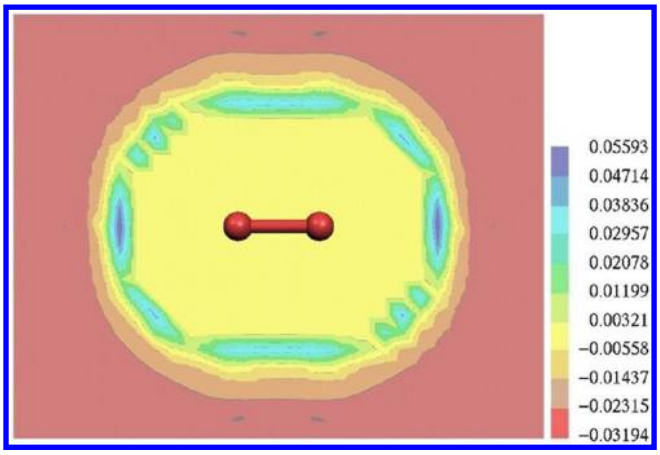

Figure 6. Contour map of the difference in the calculated Born−Oppenheimer interaction energies between an argon atom and Br_2 calculated at the CCSD(T)(full)/aug-cc-pCVQZ and EXXRPA+@dRPA/aug-cc-pCVQZ levels of theory. The color scale (interaction energies in kcal mol^{-1}) is shown on the right. The central repulsive area automatically has a zero difference because repulsive energies were set to zero for both levels.

dominates the weaker and very short-range dispersion attraction. This suggests that the ability of dispersion-corrected functionals to reproduce the binding patterns seen here should be quite sensitive to the function used to damp the interaction at short range, as confirmed by the good performance of B3LYP-D3(bj). It also suggests that a simple modification of the isotropic Lennard-Jones potential to make the van der Waals radius for the repulsive term anisotropic would help reproduce the energy hypersurfaces found here in classical force fields. Since the σ-hole and polar flattening lie in the same direction as the maximum polarizability, the happy coincidence that polar flattening promotes the correct pattern of dispersion interaction may be quite general. Thus, not only the electrostatic interaction and polarization but also dispersion contribute to the observed directionality of halogen and other σ-hole bonds.

Our results are not only consistent with the "Coulomb (including polarization) + dispersion" view[9−18,38,39] of σ-hole bonding but also suggest that polar flattening results in an enhanced dispersion contribution to σ-hole bonding. As always, however, dissecting these contributions is difficult, as they have the same directional dependence.

At least for the systems observed here, MP2(fc)/aug-cc-pVDZ (or pVTZ for BrF) appears to be an economical alternative to the reference CCSD(T)(fc) calculations. Limiting the size of the basis set prevents MP2 from overestimating the binding interaction.

Similarly, CCSD(T)(fc)/aug-cc-pVTZ calculations perform as well as CCSD(T)(fc)/aug-cc-pVQZ at a lower cost. However, the performance is degraded significantly if only CCSD is used.

Finally, the excellent performance of the EXXRPA+@EXX and EXXRPA+@dRPA calculations confirms that "next generation" density-functional theory is well able to reproduce both the magnitudes of dispersion interactions and the topologies of interaction energy hypersurfaces that are dominated by dispersion.

■ ASSOCIATED CONTENT

Ⓢ Supporting Information

CCSD(T)(fc) plots at the different basis set levels for the three dihalogens. Geometries used for interaction energy calculation and the resultant interaction energies. Plots of Br_2−Ar at the different levels of theory. Difference plots of Br_2−Ar at the different levels of theory relative to the reference level CCSD(T)(fc)/aug-cc-pVQZ. Computational details of EXXRPA+ calculations. Plots of the three dihalogens at the CCSD(T)(full)/aug-cc-pCVQZ, EXXRPA+@EXX(full)/aug-cc-pCVQZ, and EXXRPA+@dRPA(full)/aug-cc-pCVQZ levels. Difference plots of Br_2−Ar at EXXRPA+@EXX(full)/aug-cc-pCVQZ and EXXRPA+@dRPA(full)/aug-cc-pCVQZ relative to the reference level CCSD(T)(full)/Aug-cc-pCVQZ. This material is available free of charge via the Internet at http://pubs.acs.org.

■ AUTHOR INFORMATION

Corresponding Author

*E-mail: Tim.Clark@chemie.uni-erlangen.de.

Notes

The authors declare no competing financial interest.

■ ACKNOWLEDGMENTS

This work was supported by the *Bundesministerium for Bildung und Forschung* (BMBF) as part of the hpCADD project (01IH11002A), by the grant of a Fellowship to AEK by the *Deutscher Akademischer Austauschdienst* and by the *Deutsche Forschungsgemeinschaft* as part of the Excellence Cluster *Engineering of Advanced Materials*. We thank Stefan Grimme for helpful discussions.

■ REFERENCES

(1) Price, S. L.; Stone, A. J. The Electrostatic Interactions in Van der waals Complexes Involving Aromatic-Molecules. *J. Chem. Phys.* **1987**, *86*, 2859−2868.

(2) Wiberg, K. B.; Rablen, P. R. Comparison of Atomic Charges Derived Via Different Procedures. *J. Comput. Chem.* **1993**, *14*, 1504−1518.

(3) Price, S. L. Applications of realistic electrostatic modelling to molecules in complexes, solids and proteins. *J. Chem. Soc., Faraday Trans.* **1996**, *92*, 2997−3008.

(4) Politzer, P.; Murray, J. S.; Concha, M. C. σ-hole bonding between like atoms; a fallacy of atomic charges. *J. Mol. Model.* **2008**, *14*, 659−665.

(5) Murray, J. S.; Politzer, P. The electrostatic potential: an overview. *WIRES: Comput. Mol. Sci.* **2011**, *1*, 153−163.

(6) Stone, A. J. *The Theory of Intermolecular Forces*; Oxford University Press: New York, 2013; pp 13−42.

(7) Plattner, N.; Bandi, T.; Doll, J. D.; Freeman, D. L.; Meuwly, M. MD simulations using distributed multipole electrostatics: Structural and spectroscopic properties of CO- and methane-containing clathrates. *Mol. Phys.* **2008**, *106*, 1675−1684.

(8) Devereux, M.; Plattner, N.; Meuwly, M. Application of Multipolar Charge Models and Molecular Dynamics Simulations to Study Stark Shifts in Inhomogeneous Electric Fields. *J. Phys. Chem. A* **2009**, *113*, 13199−13209.

(9) Brinck, T.; Murray, J. S.; Politzer, P. Surface Electrostatic Potentials of Halogenated Methanes as Indicators of Directional Intermolecular Interactions. *Int. J. Quantum Chem.* **1992**, *44* (S19), 57−64.

(10) Auffinger, P.; Hays, F. A.; Westhof, E.; Ho, P. S. Halogen bonds in biological molecules. *Proc. Natl. Acad. Sci. U. S. A.* **2004**, *101*, 16789−16794.

(11) Awwadi, F. F.; Willett, R. D.; Peterson, K. A.; Twamley, B. The nature of halogen ... halogen synthons: Crystallographic and theoretical studies. *Chem.—Eur. J.* **2006**, *12*, 8952−8960.

(12) Clark, T.; Hennemann, M.; Murray, J. S.; Politzer, P. Halogen bonding: the σ-hole. *J. Mol. Model.* **2007**, *13*, 291−296.

(13) Cabot, R.; Hunter, C. A. Non-covalent interactions between iodoperfluorocarbons and hydrogen bond acceptors. *Chem. Commun.* **2009**, 2005−2007.

(14) Mohajeri, A.; Pakiari, A. H.; Bagheri, N. Theoretical studies on the nature of bonding in σ-hole complexes. *Chem. Phys. Lett.* **2009**, *467*, 393−397.
(15) Politzer, P.; Murray, J. S.; Clark, T. Halogen bonding: an electrostatically-driven highly directional noncovalent interaction. *Phys. Chem. Chem. Phys.* **2010**, *12*, 7748−7757.
(16) Politzer, P.; Riley, K. E.; Bulat, F. A.; Murray, J. S. Perspectives on halogen bonding and other sigma-hole interactions: Lex parsimoniae (Occam's Razor). *Comput. Theor. Chem.* **2012**, *998*, 2−8.
(17) Clark, T. σ-Holes. *WIRES: Comput. Mol. Sci.* **2013**, *3*, 13−20.
(18) Politzer, P.; Murray, J. S. Halogen Bonding: An Interim Discussion. *ChemPhysChem* **2013**, *14*, 278−294.
(19) Politzer, P.; Murray, J. S.; Clark, T. Halogen bonding and other σ-hole interactions: a perspective. *Phys. Chem. Chem. Phys.* **2013**, [online] DOI: 10.1039/C3CP00054K.
(20) Legon, A. C.; Millen, D. J. Angular Geometries and Other Properties of Hydrogen-Bonded Dimers - a Simple Electrostatic Interpretation of the Success of the Electron-Pair Model. *Chem. Soc. Rev.* **1987**, *16*, 467−498.
(21) Shields, Z. P.; Murray, J. S.; Politzer, P. Directional Tendencies of Halogen and Hydrogen Bonds. *Int. J. Quantum Chem.* **2010**, *110*, 2823−2832.
(22) Hennemann, M.; Murray, J. S.; Politzer, P.; Riley, K. E.; Clark, T. Polarization-induced σ-holes and hydrogen bonding. *J. Mol. Model.* **2012**, *18*, 2461−2469.
(23) Ibrahim, M. A. A. AMBER Empirical Potential Describes the Geometry and Energy of Noncovalent Halogen Interactions Better than Advanced Semiempirical Quantum Mechanical Method PM6-DH2X. *J. Phys. Chem. B* **2012**, *116*, 3659−3669.
(24) Kolar, M.; Hobza, P. On Extension of the Current Biomolecular Empirical Force Field for the Description of Halogen Bonds. *J. Chem. Theory Comput.* **2012**, *8*, 1325−1333.
(25) Carter, M.; Rappe, A. K.; Ho, P. S. Scalable Anisotroplic Shape and Electrostatic Models for Biological Bromine Halogen Bonds. *J. Chem. Theory Comput.* **2012**, *8*, 2461−2473.
(26) Jorgensen, W. L.; Schyman, P. Treatment of Halogen Bonding in the OPLS-AA Force Field: Application to Potent Anti-HIV Agents. *J. Chem. Theory Comput.* **2012**, *8*, 3895−3901.
(27) Stone, A. J.; Tong, C. S. Anisotropy of Atom-Atom Repulsions. *J. Comput. Chem.* **1994**, *15*, 1377−1392.
(28) (a) Williams, G. J.; Stone, A. J. Distributed dispersion: A new approach. *J. Chem. Phys.* **2003**, *119*, 4620−4628. (b) Steinmann, S. N.; Corminboeuf, C. Comprehensive Bench marking of a Density-Dependent Dispersion Correction. *J. Chem. Theory Comput.* **2011**, *7*, 3567−3577.
(29) (a) Conway, A.; Murrell, J. N. Exchange Energy between Neon Atoms. *Mol. Phys.* **1974**, *27*, 873−878. (b) Wagner, A. F.; Das, G.; Wahl, A. C. Calculated Long-Range Interactions and Low-Energy Scattering of Ar-H. *J. Chem. Phys.* **1974**, *60*, 1885−1893. (c) Hepburn, J.; Scoles, G.; Penco, R. Simple but Reliable Method for Prediction of Intermolecular Potentials. *Chem. Phys. Lett.* **1975**, *36*, 451−456. (d) Ahlrichs, R.; Penco, R.; Scoles, G. Intermolecular Forces in Simple Systems. *Chem. Phys.* **1977**, *19*, 119−130. (e) Clementi, E.; Corongiu, G. Van der Waals interaction energies of helium, neon, and argon with naphthalene. *J. Phys. Chem. A* **2001**, *105*, 10379−10383.
(30) Grimme, S. Semiempirical GGA-type density functional constructed with a long-range dispersion correction. *J. Comput. Chem.* **2006**, *27*, 1787−1799.
(31) Grimme, S.; Antony, J.; Schwabe, T.; Muck-Lichtenfeld, C. Density functional theory with dispersion corrections for supramolecular structures, aggregates, and complexes of (bio)organic molecules. *Org. Biomol. Chem.* **2007**, *5*, 741−758.
(32) Grimme, S. Density functional theory with London dispersion corrections. *WIRES: Comput. Mol. Sci.* **2011**, *1*, 211−228.
(33) Rezac, J.; Hobza, P. Advanced Corrections of Hydrogen Bonding and Dispersion for Semiempirical Quantum Mechanical Methods. *J. Chem. Theory Comput.* **2012**, *8*, 141−151.
(34) Martin, B.; Clark, T. Dispersion treatment for NDDO-based semiempirical MO techniques. *Int. J. Quantum Chem.* **2006**, *106*, 1208−1216.
(35) (a) Rinaldi, D.; Rivail, J. L. Molecular Polarizability and Dielectric Effect of Medium in Liquid-Phase - Theoretical Study of Water Molecule and Its Dimers. *Theor. Chim. Acta* **1973**, *32*, 57−70. (b) Rinaldi, D.; Rivail, J. L. Calculation of Molecular Electronic Polarizabilities - Comparison of Different Methods. *Theor. Chim. Acta* **1974**, *32*, 243−251.
(36) Schürer, G.; Gedeck, P.; Gottschalk, M.; Clark, T. Accurate parametrized variational calculations of the molecular electronic polarizability by NDDO-based methods. *Int. J. Quantum Chem.* **1999**, *75*, 17−31.
(37) Martin, B.; Gedeck, P.; Clark, T. Additive NDDO-based atomic polarizability model. *Int. J. Quantum Chem.* **2000**, *77*, 473−497.
(38) Fiedler, L.; Gao, J. L.; Truhlar, D. G. Polarized Molecular Orbital Model Chemistry. 1. Ab Initio Foundations. *J. Chem. Theory Comput.* **2011**, *7*, 852−856.
(39) Riley, K. E.; Hobza, P. Investigations into the nature of halogen bonding including symmetry adapted perturbation theory analyses. *J. Chem. Theory Comput.* **2008**, *4*, 232−242.
(40) Riley, K.; Murray, J.; Fanfrlík, J.; Řezáč, J.; Solá, R.; Concha, M.; Ramos, F.; Politzer, P. Halogen bond tunability II: the varying roles of electrostatic and dispersion contributions to attraction in halogen bonds. *J. Mol. Model.* **2013**, *19*, [online] DOI: 10.1007/s00894-012-1428-x.
(41) Arunan, E.; Desiraju, G. R.; Klein, R. A.; Sadlej, J.; Scheiner, S.; Alkorta, I.; Clary, D. C.; Crabtree, R. H.; Dannenberg, J. J.; Hobza, P.; Kjaergaard, H. G.; Legon, A. C.; Mennucci, B.; Nesbitt, D. J. Defining the hydrogen bond: An account (IUPAC Technical Report). *Pure Appl. Chem.* **2011**, *83*, 1619−1636.
(42) Murray, J. S.; Riley, K. E.; Politzer, P.; Clark, T. Directional Weak Intermolecular Interactions: σ-Hole Bonding. *Aust. J. Chem.* **2010**, *63*, 1598−1607.
(43) Hobza, P.; Zahradnik, R.; Muller-Dethlefs, K. The world of non-covalent interactions: 2006. *Collect. Czech. Chem. Commun.* **2006**, *71*, 443−531.
(44) Zhao, Y.; Truhlar, D. G. The M06 suite of density functionals for main group thermochemistry, thermochemical kinetics, noncovalent interactions, excited states, and transition elements: two new functionals and systematic testing of four M06-class functionals and 12 other functionals. *Theor. Chem. Acc.* **2008**, *120*, 215−241.
(45) Scuseria, G. E.; Janssen, C. L.; Schaefer, H. F. An Efficient Reformulation of the Closed-Shell Coupled Cluster Single and Double Excitation (CCSD) Equations. *J. Chem. Phys.* **1988**, *89*, 7382−7387.
(46) Pople, J. A.; Head-Gordon, M.; Raghavachari, K. Quadratic Configuration-Interaction - a General Technique for Determining Electron Correlation Energies. *J. Chem. Phys.* **1987**, *87*, 5968−5975.
(47) (a) Krishnan, R.; Pople, J. A. Approximate 4th-Order Perturbation-Theory of Electron Correlation Energy. *Int. J. Quantum Chem.* **1978**, *14*, 91−100. (b) Krishnan, R.; Frisch, M. J.; Pople, J. A. Contribution of Triple Substitutions to the Electron Correlation-Energy in 4th Order Perturbation-Theory. *J. Chem. Phys.* **1980**, *72*, 4244−4245.
(48) (a) Frisch, M. J.; Head-Gordon, M.; Pople, J. A. A Direct MP2 Gradient-Method. *Chem. Phys. Lett.* **1990**, *166*, 275−280. (b) Frisch, M. J.; Head-Gordon, M.; Pople, J. A. Semidirect Algorithms for the MP2 Energy and Gradient. *Chem. Phys. Lett.* **1990**, *166*, 281−289. (c) Head-Gordon, M.; Head-Gordon, T. Analytic MP2 Frequencies without 5th-Order Storage - Theory and Application to Bifurcated Hydrogen-Bonds in the Water Hexamer. *Chem. Phys. Lett.* **1994**, *220*, 122−128. (d) Head-Gordon, M.; Pople, J. A.; Frisch, M. J. MP2 Energy Evaluation by Direct Methods. *Chem. Phys. Lett.* **1988**, *153*, 503−506. (e) Møller, C.; Plesset, M. S. Note on an Approximation Treatment for Many-Electron Systems. *Phys. Rev.* **1934**, *46*, 618−622. (f) Saebo, S.; Almlof, J. Avoiding the Integral Storage Bottleneck in LCAO Calculations of Electron Correlation. *Chem. Phys. Lett.* **1989**, *154*, 83−89.
(49) (a) Dunning, T. H. Gaussian-Basis Sets for Use in Correlated Molecular Calculations 0.1. The Atoms Boron through Neon and Hydrogen. *J. Chem. Phys.* **1989**, *90*, 1007−1023. (b) Kendall, R. A.;

Dunning, T. H.; Harrison, R. J. Electron-Affinities of the 1st-Row Atoms Revisited - Systematic Basis-Sets and Wave-Functions. *J. Chem. Phys.* **1992**, *96*, 6796−6806. (c) Woon, D. E.; Dunning, T. H. Gaussian-Basis Sets for Use in Correlated Molecular Calculations. 3. The Atoms Aluminum through Argon. *J. Chem. Phys.* **1993**, *98*, 1358−1371.

(50) Grimme, S.; Antony, J.; Ehrlich, S.; Krieg, H. A consistent and accurate ab initio parametrization of density functional dispersion correction (DFT-D) for the 94 elements H-Pu. *J. Chem. Phys.* **2010**, *132*, 154104.

(51) Becke, A. D. Density-Functional Thermochemistry. 3. The Role of Exact Exchange. *J. Chem. Phys.* **1993**, *98*, 5648−5652.

(52) Goerigk, L.; Grimme, S. A thorough benchmark of density functional methods for general main group thermochemistry, kinetics, and noncovalent interactions. *Phys. Chem. Chem. Phys.* **2011**, *13*, 6670−6688.

(53) Chai, J. D.; Head-Gordon, M. Long-range corrected hybrid density functionals with damped atom-atom dispersion corrections. *Phys. Chem. Chem. Phys.* **2008**, *10*, 6615−6620.

(54) Peterson, K. A.; Dunning, T. H. Accurate correlation consistent basis sets for molecular core-valence correlation effects: The second row atoms Al-Ar, and the first row atoms B-Ne revisited. *J. Chem. Phys.* **2002**, *117*, 10548−10560.

(55) Bleiziffer, P.; He*β*elmann, A.; Görling, A. Resolution of identity approach for the Kohn-Sham correlation energy within the exact-exchange random-phase approximation. *J. Chem. Phys.* **2012**, *136*, 134102.

(56) He*β*elmann, A.; Görling, A. Random phase approximation correlation energies with exact Kohn-Sham exchange. *Mol. Phys.* **2010**, *108* (3−4), 359−372.

(57) He*β*elmann, A.; Görling, A. Correct Description of the Bond Dissociation Limit without Breaking Spin Symmetry by a Random-Phase-Approximation Correlation Functional. *Phys. Rev. Lett.* **2011**, *106*, 093001.

(58) He*β*elmann, A.; Görling, A. Random-phase approximation correlation methods for molecules and solids. *Mol. Phys.* **2011**, *109*, 2473−2500.

(59) Görling, A. Orbital- and state-dependent functionals in density-functional theory. *J. Chem. Phys.* **2005**, *123*, 062203.

(60) Langreth, D. C.; Perdew, J. P. Exchange-Correlation Energy of a Metallic Surface. *Solid State Commun.* **1975**, *17*, 1425−1429.

(61) Langreth, D. C.; Perdew, J. P. Exchange-Correlation Energy of a Metallic Surface - Wave-Vector Analysis. *Phys. Rev. B* **1977**, *15*, 2884−2901.

(62) Bleiziffer, P.; He*β*elmann, A.; Görling, A. Efficient self-consistent treatment of electron correlation within the random phase approximation. Manuscript in preparation.

(63) Frisch, M. J.; Trucks, G. W.; Schlegel, H. B.; Scuseria, G. E.; Robb, M. A.; Cheeseman, J. R.; Scalmani, G.; Barone, V.; Mennucci, B.; Petersson, G. A.; Nakatsuji, H.; Caricato, M.; Li, X.; Hratchian, H. P.; Izmaylov, A. F.; Bloino, J.; Zheng, G.; Sonnenberg, J. L.; Hada, M.; Ehara, M.; Toyota, K.; Fukuda, R.; Hasegawa, J.; Ishida, M.; Nakajima, T.; Honda, Y.; Kitao, O.; Nakai, H.; Vreven, T.; Montgomery, J. A., Jr.; Peralta, J. E.; Ogliaro, F.; Bearpark, M.; Heyd, J. J.; Brothers, E.; Kudin, K. N.; Staroverov, V. N.; Kobayashi, R.; Normand, J.; Raghavachari, K.; Rendell, A.; Burant, J. C.; Iyengar, S. S.; Tomasi, J.; Cossi, M.; Rega, N.; Millam, J. M.; Klene, M.; Knox, J. E.; Cross, J. B.; Bakken, V.; Adamo, C.; Jaramillo, J.; Gomperts, R.; Stratmann, R. E.; Yazyev, O.; Austin, A. J.; Cammi, R.; Pomelli, C.; Ochterski, J. W.; Martin, R. L.; Morokuma, K.; Zakrzewski, V. G.; Voth, G. A.; Salvador, P.; Dannenberg, J. J.; Dapprich, S.; Daniels, A. D.; Farkas, Ö.; Foresman, J. B.; Ortiz, J. V.; Cioslowski, J.; Fox, D. J. *Gaussian 09*, revision A.02; Gaussian, Inc.: Wallingford, CT, 2009.

(64) Werner, H.-J.; Knowles, P. G.; Knizia, G.; Manby, F. R.; Schütz, M.; Celani, P.; Korona, T.; Lindh, R.; Mitrushenkov, A.; Rauhut, G.; Shamasundar, K. R.; Adler, T. B.; Amos, R. D.; Bernhardsson, A.; Berning, A.; Cooper, D. L.; Deegan, M. J. O.; Dobbyn, A. J.; Eckert, F.; Goll, E.; Hampel, C.; Hesselmann, A.; Hetzer, G.; Hrenar, T.; Jansen, G.; Köppl, C.; Liu, Y.; Lloyd, A. W.; Mata, R. A.; May, A. J.; McNicholas, S. J.; Meyer, W.; Mura, M. E.; Nicklaß, A.; O'Neill, D. P.; Palmieri, P.; Peng, D.; Pflüger, K.; Pitzer, R.; Reiher, M.; Shiozaki, T.; Stoll, H.; Stone, A. J.; Tarroni, R.; Thorsteinsson, T.; Wang, M. *MOLPRO*, version 2010.2; Cardiff University: Cardiff, U. K.; Universität Stuttgart: Stuttgart, Germany, 2010. http://www.molpro.net.

(65) Grimme, S.; Antony, J.; Ehrlich, S.; Krieg, H. DFT-D3 - A dispersion correction for DFT-functionals. http://toc.uni-muenster.de/DFTD3/ (accessed January 15th 2013).

(66) Stevens, E. D. Experimental Electron-Density Distribution of Molecular Chlorine. *Mol. Phys.* **1979**, *37*, 27−45.

(67) Nyburg, S. C. Polar Flattening - Non-Spherical Effective Shapes of Atoms in Crystals. *Acta Crystallogr., Sect. A* **1979**, *35*, 641−645.

(68) Bilewicz, E.; Rybarczyk-Pirek, A. J.; Dubis, A. T.; Grabowski, S. J. Halogen bonding in crystal structure of 1-methylpyrrol-2-yl trichloromethyl ketone. *J. Mol. Struct.* **2007**, *829*, 208−211.

(69) Lennard-Jones, J. E. On the Determination of Molecular Fields. II. From the Equation of State of a Gas. *Proc. R. Soc. London, Ser. A* **1924**, *106*, 463−477.

(70) Stote, R. H.; Adelman, S. A. Theory of Vibrational-Energy Relaxation in Liquids - Diatomic Solutes in Monatomic Solvents. *J. Chem. Phys.* **1988**, *88*, 4415−4420.

(71) He, X.; Fusti-Molnar, L.; Cui, G. L.; Merz, K. M. Importance of Dispersion and Electron Correlation in ab Initio Protein Folding. *J. Phys. Chem. B* **2009**, *113*, 5290−5300.

(72) Cybulski, S. M.; Chalasinski, G.; Moszynski, R. On decomposition of second-order Møller-Plesset supermolecular interaction energy and basis set effects. *J. Chem. Phys.* **1990**, *92*, 4357−4363.

(73) Chalasinski, G.; Szczesniak, M. M. On the Connection between the Supermolecular Moller-Plesset Treatment of the Interaction Energy and the Perturbation-Theory of Intermolecular Forces. *Mol. Phys.* **1988**, *63*, 205−224.

(74) Grimme, S. Improved second-order Moller-Plesset perturbation theory by separate scaling of parallel- and antiparallel-spin pair correlation energies. *J. Chem. Phys.* **2003**, *118*, 9095−9102.

(75) Löwdin, P.-O. Twenty-five years of Sanibel symposia: A brief historic and scientific survey. *Int. J. Quantum Chem.* **1985**, *28* (S19), 19−37.